

Optical effects of dust particles of different shapes

M. Kocifaj and I. Kapišinský

Astronomical Institute of the Slovak Academy of Sciences, Interplanetary Matter Division, Dúbravská cesta 9, 842 28 Bratislava, The Slovak Republic

Received: May 13, 1996

Abstract. Cosmic dust dynamics depends not only on many nongravitational effects, but also on the physical and optical properties of particles. In this connection important optical factors such as the complex refractive index m and the efficiency factor for radiation pressure Q_{pr} , strongly depend on the shape of particle. The paper presents precise calculations of the Q_{pr} factor and scattering phase functions $p(\theta_s, \varphi_s)$ applying the Discrete Dipole Approximation method to six particles of different shapes (sphere, cylinder, ellipsoid, hexagonal prism, rectangular target, tetrahedron). The high variability of the Q_{pr} and $p(\theta_s, \varphi_s)$ values for some specially shaped particle models, presented in both tabulated and graphical forms, confirms the strong dependence of the dynamical-optical factors on the shape parameter. This dependence is more significant for particles of irregular shape, especially for cylinders in our particle sample.

Key words: cosmic dust particles – radiation pressure – radiation scattering – particle refractive index

1. Introduction

Fine, micron and submicron particles in the atmosphere and space are of interest in geological, dynamical and many astronomical phenomena. Interplanetary dust particles (IDPs) seem to be largely responsible for zodiacal light, and their presence raises questions concerning their nature and their source. The Cosmic Dust Program has been run by NASA since 1981 to collect cosmic dust particles directly ("in situ") from the Earth's stratosphere. A statistical analysis of this collection experiment over almost fifteen years shows that the percentage of dust of true cosmic origin is roughly 30 % (Kapišinský, 1992). These particles are the best available samples of IDPs (Walker, 1985), and they are also very suitable for studying their physical and optical properties with respect to dust dynamics in general. Therefore, we have also studied them under laboratory conditions using a variety of analytical techniques.

One of the important factors (optical constants) in estimating the efficiency factor for radiation pressure is the complex refractive index of particles

$m = m_r - im_i$, where m_r and m_i are the real and imaginary part of the refractive index, respectively. The scattering and absorption of an electromagnetic plane wave incident on a spherical, homogeneous, isotropic particle is a classical problem whose complete solution was independently obtained by Mie (1908) and Debye (1909). The solution is now commonly referred to as the "Mie theory". Of course, the shape of the particles also play a very important role in their dynamics, but for simplicity, dust grains are often assumed to be spherical. But, as a matter of fact, the percentage of irregularly shaped cosmic particles is roughly 87 (See Tab. 2 and conclusion 5C in Kapišinský, 1992). Therefore, the informations about particle shape and particle refractive index $m(\lambda)$ (for wavelength range from far UV to far IR) are necessary for a more reliable estimation of the optical characteristics of true IDPs. However, as concerns m , it is hard to obtain all reasonable data of m for existing IDPs. Especially, we cannot prepare the laboratory data of m for all kinds of heterogeneous dust samples due to their great degree of contamination. Therefore, a theoretical study is required and modelling methods have to be used in this field of research.

In this paper we want to show the changes of optical parameters of the particles in dependence on their shape. Of course, IDP particles have their own size and shape distributions, chemical composition and optical properties (Flynn, 1994). The experiments in the stratosphere showed that the particle number per unit weight of air remained nearly constant, i.e. there was a nearly constant mixing ratio (Cadle, 1966). It is evident, if a particle source is above the atmosphere, that the mixing ratio and size distribution will be independent of altitude, while if the source is in the lower atmosphere or at the Earth's surface, the mixing ratio and size distribution will be altitude dependent in the stratosphere. The first serious studies concluded that the source of these particles must be at least above 85 km and estimated the downward mass flux of particles 0.5 to 2 μm in diameter to be 6.106ρ metric tons per year over the Earth, where ρ is the average density of the dust particles. As mentioned above, the collection of dust particles in the Earth's stratosphere, within the scope of the Cosmic Dust Program in the NASA Johnson Space Center, shows that at least about 30 % of these particles are of cosmic origin. The important part of the cosmic dust particles floating in the stratosphere is of micron and submicron range, and the size distribution of their origin sources is assumed in the form of Junge's distribution $f(r) \approx Ar^{-n}$ with parameter n approximately equal to 2.8 (r is a particle radius) (Cadle, 1966; Kocifaj, 1994). The dynamics of IDPs of submicron range is in the high degree predicted by many nongravitational effects i.e. mainly by their interaction with solar radiation (Kapišinský, 1984). Light scattering by particles (micron and submicron sizes) cannot be calculated using the Rayleigh or geometric optics approximations. The basic Maxwell's equations must be solved in general case, i.e. for particles of arbitrary shape and composition. Unfortunately, the rigorous analytical solution is known only for special particle types: i.e. for spherical, homogeneous, and isotropic particle (Mie, 1908), for particles very small compared to the incident

wavelength, infinite cylinders, and, homogeneous isotropic spheroids. The known approach to solve the light scattering by nonspherical particles is so-called T-matrix method (Mishchenko, 1991; Mishchenko and Travis, 1994a; Mishchenko and Travis, 1994b; Mishchenko and Travis, 1994c). But this method is not suitable for particle surfaces with deep concavities. The perturbation method is also limited by certain finite values of refractive indices (Barber and Yeh, 1975; Wang and Barber, 1979; Wang et al., 1979). We are applying the Discrete Dipole Approximation (DDA) method which was successful used to calculate the optical effects of interplanetary grains of different shapes (Draine, 1988; Draine and Goodman, 1993; Draine and Flatau, 1994a; Lumme and Rahola, 1994).

On the basis of precise calculations of light scattering by different shaped particles we want to show in this paper that often used simply spherical approximation extend to chance oriented nonspherical particles leads to inadequate evaluation of particle motion in the space. The DDA method was used for numerical calculations. Moreover, the original well-known assumption that the particles can be considered as total absorbing or total reflecting objects is not quite acceptable. The comparison of results for multicomponent particles and homogeneous particles of identical volume and shape leads also to the different conclusions (e.g. for materials with refractive indices strongly dependent on incident wavelength). This was one of many arguments to start the dust study also at our laboratory in order to obtain more reliable input data which is necessary for our theoretical research in the field of dust dynamics. First series of papers dealing with laboratory analyses of dust samples were published recently (Kapišinský et al., 1994, 1995, 1996).

2. Scattering and absorption characteristics for certain particle types

2.1. Theoretical background

Motion of small particles in the interplanetary space is connected with such optical characteristics as scattering and absorption cross sections C_{sca} and C_{abs} , respectively, and phase function $p(\theta_s, \varphi_s)$, where θ_s and φ_s are scattering angle and azimuth angle which gives the orientation of the scattering plane, respectively. These functions are defined for a far zone as follows:

$$C_{sca} = \int_{4\pi} \frac{|\mathbf{T}|}{k^2 |\mathbf{E}_i|^2} d\Omega, \quad (1)$$

$$C_{ext} = \frac{4\pi}{k^2 |\mathbf{E}_i|^2} Re \{ (\mathbf{E}_i^* \cdot \mathbf{T})_{\theta_s=0} \}, \quad (2)$$

where

$$C_{abs} = C_{ext} - C_{sca}, \quad (3)$$

and

$$p(\theta_s, \varphi_s) = \frac{|\mathbf{T}|^2}{k^2 |\mathbf{E}_i|^2 C_{sca}}, \quad (4)$$

where $\mathbf{T} = E_x \mathbf{X} + E_y \mathbf{Y}$, \mathbf{X} and \mathbf{Y} are vector-amplitudes of a scattered radiation for x- and y-polarized states, \mathbf{E}_i describes the incident radiation field, k is a wave vector and $d\Omega = \sin\theta_s d\theta_s d\varphi_s$. The effectivity of radiation influence on dust particles motion is evaluated by the efficiency factor for radiation pressure Q_{pr} :

$$Q_{pr} = Q_{ext} - \langle \cos\theta_s \rangle Q_{sca}, \quad (5)$$

where Q_{ext} and Q_{sca} are the efficiency factors for extinction and scattering, respectively, and $\langle \cos\theta_s \rangle$ is the asymmetry factor which gives the proportional part of the total forward momentum carried by the scattered radiation. The projections of scattered radiation momentum perpendicular to previous projection and constructed by phase functions corresponds with the changes of spiraling particle motion in the interplanetary space. The complete equation of motion can be expressed as follows (Klačka and Kocifaj, 1994):

$$\begin{aligned} \frac{d\mathbf{v}}{dt} = \frac{S}{mc} & \left\{ \left[C_{ext} - C_{sca} \int_{4\pi} p(\theta_s, \varphi_s) \cos\theta_s d\Omega \right] \times \right. \\ & \times \left[\left(1 - \mathbf{v} \frac{\mathbf{S}_i}{c} \right) \mathbf{S}_i - \frac{\mathbf{v}}{c} \right] - \left(1 - 2\mathbf{v} \frac{\mathbf{S}_i}{c} \right) C_{sca} \times \\ & \times \left[\mathbf{e}_T \int_{4\pi} p(\theta_s, \varphi_s) \sin\theta_s \cos\varphi_s d\Omega + \mathbf{e}_N \int_{4\pi} p(\theta_s, \varphi_s) \sin\theta_s \sin\varphi_s d\Omega \right] - \\ & \left. - \mathbf{S}_i C_{sca} \frac{\mathbf{v} \cdot \mathbf{e}_T}{c} \int_{4\pi} p(\theta_s, \varphi_s) \sin\theta_s \cos\varphi_s d\Omega \right\}, \quad (6) \end{aligned}$$

where \mathbf{S}_i denotes the incident radiation, c is the light velocity, \mathbf{v} particle velocity, m particle mass, Ω solid angle, t time, \mathbf{e}_T a unit vector transverse to the radial vector \mathbf{S}_i , $\mathbf{e}_T = \mathbf{S}_i \times \mathbf{e}_N$ and S is defined by Eq. (10) in paper quoted above.

2.2. Numerical results

The calculations of the characteristics of scattered light by differently shaped particles were based on DDA. The wavelength $0.55 \mu\text{m}$ of the incident radiation of the maximum in the solar spectrum energy distribution was used in the model calculations. The optical properties of the particles correspond to typical interplanetary material (silicate grain). The particle refractive index $m(\lambda = 0.55 \mu\text{m}) = 1.48 - 2.8 \times 10^{-5}i$ was taken into account (Mukai, 1989). The particle effective radius r_{eff} , defined as the radius of a sphere of equal volume, i.e. a sphere of volume Nd^3 , where d is the lattice spacing and N is the number of occupied (i.e. non-vacuum) lattice sites in the target (Draine and Flatau, 1994b) was chosen from the submicron range and set to $0.5 \mu\text{m}$. The calculation results

were obtained for six particle types with defined characteristics (Table 1) and for 25 orientations. The particle is assumed to have two vectors \mathbf{a}_1 and \mathbf{a}_2 embedded in it, \mathbf{a}_2 being perpendicular to \mathbf{a}_1 . The particle orientation in the lab frame was defined by three angles: β , θ , and φ . The particle is oriented in such a way that polar angles θ and φ specify the direction of \mathbf{a}_1 relative to polar axis \mathbf{e}_x , where the $\mathbf{e}_x - \mathbf{e}_y$ plane has $\varphi = 0^\circ$. The particle is assumed to rotate around \mathbf{a}_1 through angle β . Incident light was assumed in two polarized states, i.e. \mathbf{e}_x (the direction of propagation of the radiation) and \mathbf{e}_y (usually the first polarization direction).

Table 1. Description of particle characteristics (according to user manual for DDSCAT V.4C by Draine and Flatau 1994b).

target	PAR1	PAR2	PAR3	Number of dipoles
Sphere	30	30	30	14328
Cylinder	32	16	1	6656
Ellipsoid	96	40	10	40272
Hexagonal prism	4000	1	1	4000
Rectangular	120	40	10	48000
Tetrahedron	35	2	2	5053

The calculation results of Q_{pr} for given particles in different orientations are presented in the Table 2. A much greater variability of Q_{pr} was observed for the hexagonal prism than for the rectangular target. The variability of Q_{pr} for tetrahedron particle is not so different from the sphere. However, the mean values of Q_{pr} for all discussed particles are very different and vary over one order of magnitude. This is a strong motivation to develop the methods for precise determination of particle shape or morphology. The simply spheroidal approximation of particle shape is not sufficient for accurate calculations of particle motion in the space.

Table 2. Q_{pr} of six studied particles obtained from 25 orientations.

target	$Q_{pr}(\text{mean})$	$Q_{pr}(\text{minimum})$	$Q_{pr}(\text{maximum})$
Sphere	1.102	1.10	1.10
Cylinder	1.022	0.39	1.21
Ellipsoid	0.765	0.31	0.96
Hexagonal prism	0.123	0.00	0.80
Rectangular	0.478	0.16	0.74
Tetrahedron	1.034	0.61	1.31

The numerical results obtained for following "motion integrals":

$$G_0 = Q_{ext} - Q_{sca} \int_{4\pi} p(\theta_s, \varphi_s) \cos\theta_s d\Omega$$

$$G_1 = Q_{sca} \int_{4\pi} p(\theta_s, \varphi_s) \sin\theta_s \cos\varphi_s d\Omega$$

$$G_2 = Q_{sca} \int_{4\pi} p(\theta_s, \varphi_s) \sin\theta_s \sin\varphi_s d\Omega$$

showed unambiguously that the projections of scattered radiation energy in directions perpendicular to the radial direction can yield sufficient values to change the predicted particle motion by the Poynting-Robertson effect (G_1 and G_2 must be at least at level 10^{-4} of G_0).

The corresponding phase functions are presented in figures 1 (sphere), 2a-c (cylinder), 3a-c (hexagonal prism), 4a-c (ellipsoid), 5a-c (rectangular target), and 6a-c (tetrahedron), respectively. The isolines are drawn in polar coordinates θ_s, φ_s , where θ_s is the angle between the incident beam and the scattered beam ($\theta_s = 0^\circ$ for forward scattering, $\theta_s = 180^\circ$ for backscattering) and azimuth angle describes the orientation of the scattering plane. The isolines were plotted on a logarithmic scale. One can see that the structure of isolines is very near to radial symmetry for cylindrical and hexagonal particles, but the range of absolute values of $p(\theta_s, \varphi_s)$ are much greater in the case of the hexagonal prism in comparison with the cylinder. Most deformations of the radially symmetric profile were detected with the tetrahedron particle. Generally it could be said that the phase function profile correlates with particle shape in orientation $\theta = 0^\circ$ (i.e. when the long axis of particle is parallel to the incident radiation). A certain radial symmetry can be observed in position $\theta = 90^\circ$ (i.e. the short axis of the particle is parallel to the incident radiation), but it is clear that this radial symmetry is relatively smaller than in the previous case. It is reflected also in ratios G_1/G_0 and G_2/G_0 . The greater the deviation from radial symmetry of the phase functions, the greater these ratios G_1/G_0 and G_2/G_0 . These ratios importantly influence the particle motion in interplanetary space. However, the particles also rotate and due to the phase functions must be averaged over orientations. The resulting motion of the particle caused by radiation pressure is connected not only with the isoline structure, but also with the distribution of the absolute amount of scattered energy. The greater the range of values $p(\theta_s, \varphi_s)$, the smaller the deflection from the radial motion of particles (the smaller the ratios G_1/G_0 or G_2/G_0). The reason for this is that the greatest amount of radiation energy is always scattered in the radial direction. The results of the calculation for non-spherical particles show that the smallest variations of the $p(\theta_s, \varphi_s)$ values were observed for the cylindrical particle (about one order for orientation $\theta = 0^\circ$ and about three orders for orientation $\theta = 90^\circ$). For other particles this is about 3-4 orders (ellipsoid, rectangular target, tetrahedron), and 7 orders (hexagonal prism). The absolute values of the phase function for the spherical particle varies over two orders.

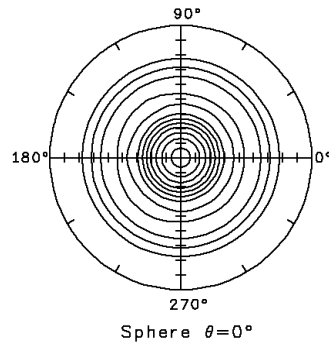


Figure 1. Izolines of the phase functions for light scattering by spherical particle. Particle radius: $0.5\mu\text{m}$, wavelength: $0.55\mu\text{m}$.

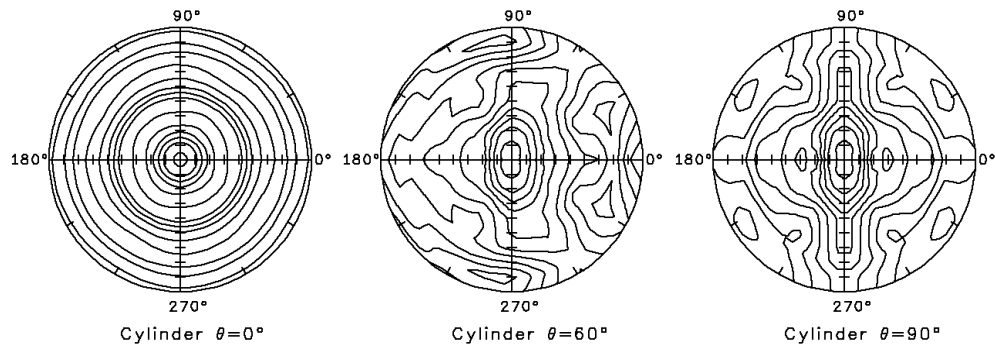


Figure 2. a-c: Izolines of the phase functions for light scattering by cylindrical particle. Particle radius: $0.5\mu\text{m}$, wavelength: $0.55\mu\text{m}$.

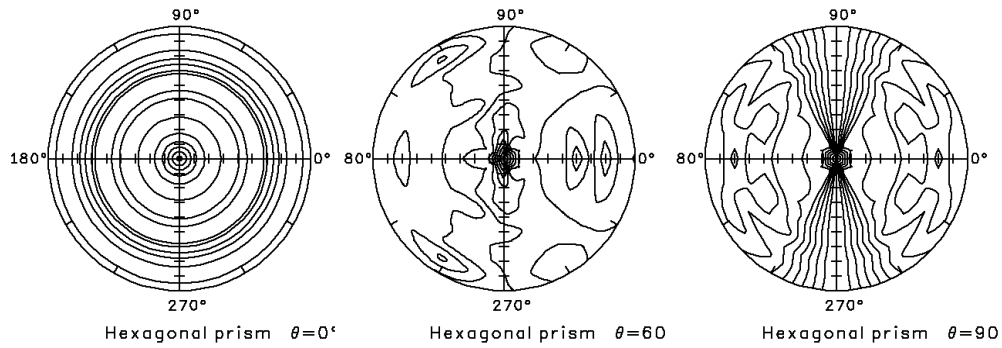


Figure 3. a-c: Izolines of the phase functions for light scattering by hexagonal particle. Particle radius: $0.5\mu\text{m}$, wavelength: $0.55\mu\text{m}$.

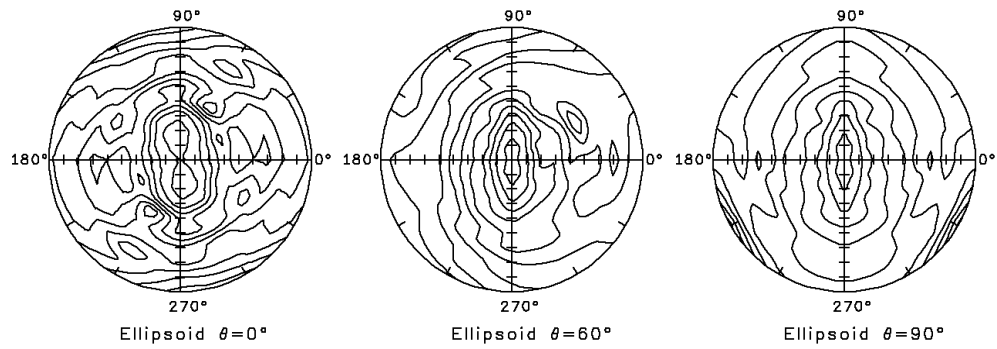


Figure 4. a-c: Isolines of the phase functions for light scattering by ellipsoidal particle. Particle radius: $0.5\mu\text{m}$, wavelength: $0.55\mu\text{m}$.

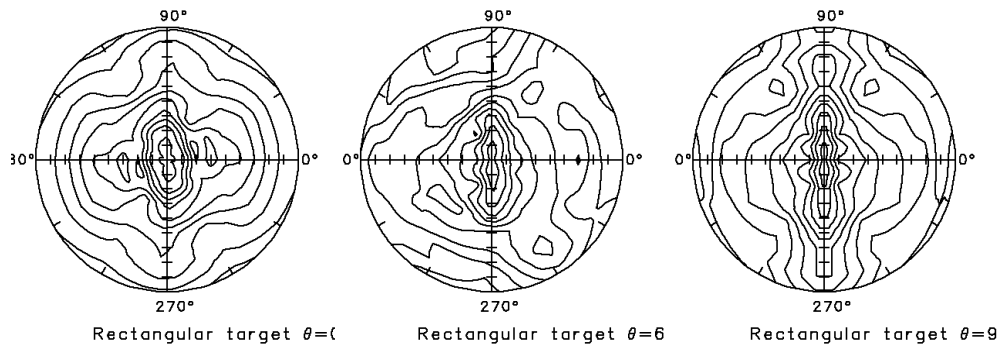


Figure 5. a-c: Isolines of the phase functions for light scattering by rectangular particle. Particle radius: $0.5\mu\text{m}$, wavelength: $0.55\mu\text{m}$.

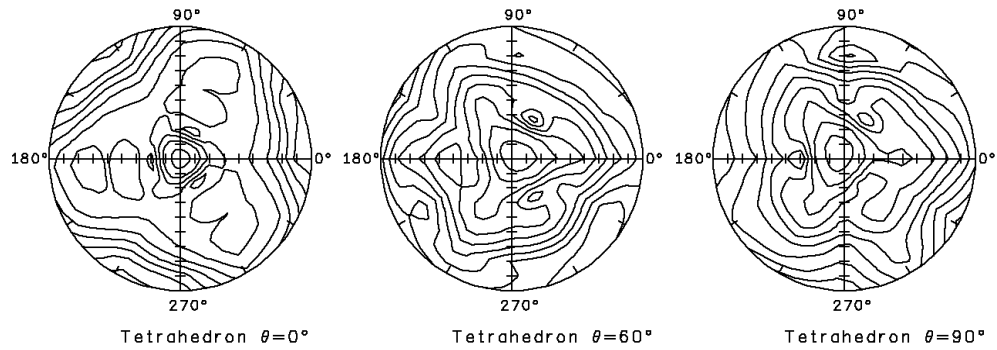


Figure 6. a-c: Isolines of the phase functions for light scattering by tetrahedron particle. Particle radius: $0.5\mu\text{m}$, wavelength: $0.55\mu\text{m}$.

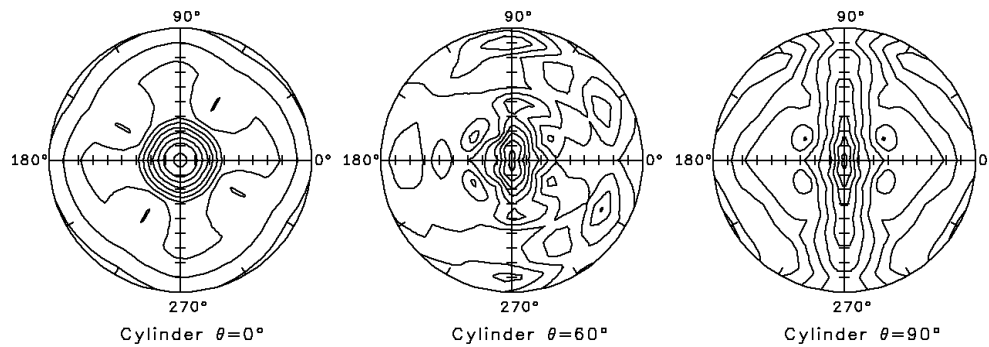


Figure 7. a-c: Isolines of the phase functions for light scattering by cylindrical particle. Particle radius: $1.0\mu m$, wavelength: $0.55\mu m$.

3. Results - Discussion

The results indicate that the cylindrical particle is the best candidate in our collection for atypical motion in interplanetary space in comparison with the classical Poynting-Robertson inspiralling motion. This effect is more significant for the cylinder whose size is close to the wavelength of incident radiation. This is shown in Figs. 2a-c, and 7a-c, which compare the phase diagrams for cylindrical particles with effective radii of $0.5\mu m$ and $1.0\mu m$, respectively. It is shown that the isolines are roughly similar (differences are detected in the case $\theta = 0^\circ$), but the range of absolute values of $p(\theta_s, \varphi_s)$ is significantly different: Fig.2a - one order and Fig. 7a - three orders, Fig. 2b - two orders and Fig. 7b - four orders, Fig. 2c - three orders and Fig. 7c - three orders.

Acknowledgements. This work has been supported by a Grant No 1051 of the Slovak Academy of Sciences. The authors are also grateful to Dr. Draine of the Princeton University Observatory for their DDSCAT codes and to Mrs. Z. Kapišinská for helping to prepare the manuscript.

References

- Barber, P.W., Yeh, C.: 1975, *App. Opt.* **14**, 2864
 Cadle, R.D.: 1966, *Particles in the atmosphere and space*, Reinhold Publ. Corp., New York
 Debye, P.: 1909, *Ann. Phys.* **30**, 57
 Draine, B.T.: 1988, *Astrophys. J.* **333**, 848
 Draine, B.T., Goodman, J.: 1993, *Astrophys. J.* **405**, 685
 Draine, B.T., Flatau, P.J.: 1994a, *J. Opt. Soc. Am. A* **11**, 1491
 Draine, B.T., Flatau, P.J.: 1994b, *User manual for DDSCAT V.4C*,
 Flynn, J.G.: 1994, *Planet. Space Sci.* **42**, 1151

- Kapišinský, I.: 1984, *Contrib. Astron. Obs. Skalnaté Pleso* **12**, 99
- Kapišinský, I.: 1992, *Contrib. Astron. Obs. Skalnaté Pleso* **22**, 215
- Kapišinský, I., Figusch, V., Hajduk, A., Ivan, J., Iždinský, K.: 1994, *Earth, Moon, Planets* **64**, 273
- Kapišinský, I., Hajduk, A., Ivan, J., Iždinský, K.: 1995, *Earth, Moon, Planets* **68**, 347
- Kapišinský, I., Hajduk, A., Ivan, J., Iždinský, K.: 1996, *Earth, Moon, Planets* **73**, 7
- Klačka, J., Kocifaj, M.: 1994, *In: Proceedings of the Conference on Astrometry and Celestial Mechanics, Poznań 13-17 Sept. 93*, 187
- Kocifaj, M.: 1994, *Stud. Geoph. Geod.* **38**, 304
- Lumme, K., Rahola, J.: 1994, *Astrophys. J.* **425**, 653
- Mie, G.: 1908, *Ann. Phys.* **25**, 377
- Mishchenko, M.I.: 1991, *J. Opt. Soc. Am. A* **8**, 871
- Mishchenko, M.I., Travis, L.D.: 1994a, *J. Quant. Spectrosc. Radiat. Transfer* **51**, 759
- Mishchenko, M.I., Travis, L.D.: 1994b, *Optics Communications* **109**, 16
- Mishchenko, M.I., Travis, L.D.: 1994c, *Appl. Optics* **30**, 7201
- Mukai, T.: 1989, *In: Evolution of interstellar dust and related topics*, Amsterdam, Oxford, New York, Tokyo, 410
- Walker, R.M.: 1985, *In: NASA Conference Publication 2403*, Maryland, 55
- Wang, D.S., Chen, H.C.H., Barber, P.W., Wyatt, P.J.: 1979, *Appl. Opt.* **18**, 2672
- Wang, D.S., Barber, P.W.: 1979, *Appl. Opt.* **18**, 1190